

**In Press (2004): Chemical Engineering Communications Manuscript No: 205-2**

**AN INTERPRETATION MODEL FOR THE UV-VIS SPECTRA OF  
MICROORGANISMS**

**Catalina E. Alupoaei**

**Luis H. García-Rubio \***

Department of Chemical Engineering, University of South Florida, Tampa, FL 33620

**Keywords:** Biosensor, Multiwavelength Spectroscopy, Absorbance, Scattering, Deconvolution, Optical properties, Mie theory, *E. coli*, *B. globigii*.

\*To whom correspondence should be addressed at: University of South Florida,  
Department of Chemical Engineering ENB 118, 4202 E. Fowler Avenue, Tampa, FL  
33620. Tel: (813) 974-5854; Fax: (813) 947-3651; email: [garcia@eng.usf.edu](mailto:garcia@eng.usf.edu)

†*Abbreviations:* Uv-vis, ultraviolet-visible; DNA, deoxyribonucleic acid; RNA,  
ribonucleic acid; DPA, dipicolinic acid; Au, absorbance units.

## **ABSTRACT**

Multiwavelength Uv-vis spectra of microorganisms and cell suspensions contain quantitative information on their properties such as number, size, shape, chemical composition, and internal structure. These properties are essential for the identification and classification of cells. The complexity of microorganisms in terms of their chemical composition and internal structure make the interpretation of their spectral signature a difficult task. In this paper a model is proposed for the interpretation of the multiwavelength spectra of microorganisms. The proposed interpretation model is based on light scattering theory, spectral deconvolution techniques, and on the approximation of the frequency dependent optical properties of the basic constituents of living organisms. The optical properties as functions of wavelength, and available literature data on the size and chemical composition of *E. coli* cells and *Bacillus globigii* spores have been used to explore the sensitivity of the calculated spectra to the model parameters. It is shown that the proposed model can reproduce the features of experimentally measured spectra. The sensitivity of the spectra to the model parameters suggests that the proposed model can be used for the quantitative deconvolution of the Uv-vis spectra in terms of critical information necessary for the detection and identification of microorganisms.

## **INTRODUCTION**

Multiwavelength ultraviolet/visible (Uv-vis) spectroscopy is a versatile, quantitative, rapid, and reliable analytical tool that has immediate applications as a biosensor for the detection, identification, and enumeration of microorganisms and cells. The sample information contained in a spectrum includes cell size, chemical composition, shape, and information on their internal structure. This information is obtained from the spectroscopic analysis of a sample measured over a broad range of wavelengths (200-900 nm) and/or with the scattered light measured at one or many different angles. The potential to extract large amounts of information from a single multiwavelength measurement makes Uv-vis spectroscopy a powerful characterization tool. In addition, process Uv-vis spectrometers and miniaturized systems, make this technique readily available for real-time in situ monitoring of biological, and environmental processes. Furthermore, a spectroscopy-based biosensor provides the added benefits of being rapid, inexpensive and relatively simple to operate.

Multiwavelength and angular scattering spectroscopy analysis of microorganisms has been reported in the literature (e.g. 1-21). Uv-vis and other spectroscopy techniques such as fluorescence, Raman and infrared have been reported and used for the estimation of the number of cells and their chemical composition, in particular, the nucleic acid and protein concentrations (1, 6, 11, 22-24). The angular scattering spectrum from cells and microorganisms has also received a great deal of attention because of the sensitivity of the angular intensity distribution to size, shape and orientation of the suspended particles (e.g. 8, 9, 11, 12 17, 18, 20, 21). More recently, polarized light scattering experiments have been used to further characterize microorganisms through sensitive elements of the

scattering matrix (2, 18, 25). The main limitations for the use of spectroscopy techniques have been both instrumental and theoretical. Commercially available light scattering instrumentation is typically designed for single wavelength operation with a goniometer or with detectors at fixed angles. To be able to discriminate between different microorganisms, considerable differences in size, shape and refractive index are necessary. This is difficult because most microorganisms have approximately the same chemical composition (i.e., water content, proteins, DNA, etc.) and as a result they have relatively small differences in refractive index (19, 20, 26). In addition, particles the size of cells and microorganisms (0.5-10  $\mu\text{m}$ ) typically forward scatter light, which means that although distinguishing features may be present at wider measurement angles, particularly with polarized light (25, 27, 28), the signal to noise ratio is not favorable. Multiwavelength transmission measurements and related turbidimetry techniques have been extensively used in biological applications ranging from the definition of standards of water quality, to measurements of the DNA content in microorganisms and cell enumeration (6, 13, 19, 22, 23, 29). However these applications have been largely limited to corrections assuming Rayleigh scattering, or to calibrations relating the optical densities at discrete wavelengths to the particle concentration. To date there have been few attempts to model the spectra to extract quantitative information on the optical properties of microorganisms. Notable exemptions are the reports by Inagaki (7), Waltham (19), Tuminello (30), and Yabushita (31, 32), who reported measurements of optical properties.

In this paper a model is proposed for the interpretation of the multiwavelength spectra of microorganisms. The proposed interpretation model is based

on light scattering theory, spectral deconvolution techniques, and on the approximation of the frequency dependent optical properties of the basic constituents of living organisms. The characteristic sets of optical properties for chromophoric groups present in microorganisms have been evaluated and are reported herein. The optical properties as functions of wavelength have been used to explore the sensitivity of the model. Several hypotheses have been tested to demonstrate the applicability of the proposed interpretation model for the deconvolution of spectra in terms of critical parameters necessary for the detection and identification of microorganisms. The experimental spectral fingerprints from *E. coli* cells, and *B. Globigii* spores are used as reference.

## **THEORETICAL BACKGROUND**

The multiwavelength transmission spectrum of particle dispersions contains information that, in principle, can be used to estimate the particle size distribution (PSD) and the chemical composition of the suspended particles. The complexity of microorganisms in terms of their chemical composition and internal structure make the interpretation of their spectral signature a very difficult task. Nevertheless, several attempts have been made to model the shape and internal structure of the cells using the Rayleigh-Debye-Gans (RDG) approximation (4, 9, 17, 20) and the anomalous diffraction, or van de Hulst approximation (13, 33, 34). The motivation in using the RDG approximation is the ability to account for shape and orientation through appropriate form factors (25, 27). The main limitation of both, the anomalous diffraction and the RDG approximation is the requirement that the refractive index ratio between the particles and the suspending medium be close to 1. For vegetative cells this is not a serious limitation. However for spores, which are highly refractile, the refractive index

ratio is no longer close to 1 and therefore the RDG approximation no longer applies. It is worth noticing that in the RDG, the absorption cross-section only depends on the particle volume and it is independent of the particle shape. Similarly, in the anomalous diffraction approximation the absorption cross section is independent of the refractive index of the particles (28).

A model for the interpretation of the Uv-vis spectra that is not often explored is Mie theory, where the volume of the microorganisms is expressed in terms of an equivalent sphere (15, 17). In addition to not having restrictions relative to the size of the particles and the values of the refractive index, there are several arguments justifying the use of the volume equivalent scattering approximation, particularly when it is used in the context of transmission measurements:

1. Particles the size of cells and microorganisms (0.5-10  $\mu\text{m}$ ) typically forward scatter light, which means that measurements in the forward direction (transmission) with the appropriate angle of acceptance will capture the majority of the scattered light as well as the attenuation due to absorption.
2. The sum rule for extinction developed for spheroids by Purcell (25, 35) suggests that, regardless of the shape of the particle, the integrated extinction (as function of wavelength) is proportional to the particle volume. Since multiwavelength transmission measurements are typically conducted over a wide range of wavelengths (200-900 nm), we can consider this proportionality to hold.
3. Independent evaluations of scattering cross-sections for complex cells such as red blood cells have shown that the extinction efficiencies calculated using rigorous form factors and the volume equivalent spherical approximations yield

comparable results (36). It has been shown (12) that the effects of the particle shape on the scattering diagrams can be compensated by changes in the refractive index. Since the refractive indices have to be estimated, the use of the spherical-equivalent approximation in combination with the refractive index estimation can be expected to yield adequate representation of the spectral features (12).

The Equation that relates the turbidity  $\tau(\lambda_o)$  measured at a given wavelength  $\lambda_o$  and the normalized particle size distribution for homogeneous particles  $f(D)$  is given by Kerker (27).

$$\tau(\lambda_o) = N_p \ell \left(\frac{\pi}{4}\right) \int_0^{\infty} Q_{ext}(m(\lambda_o), D) D^2 f(D) dD \quad (1)$$

Where  $\ell$  is the pathlength,  $D$  represents the particle diameter,  $Q_{ext}$  corresponds to the Mie extinction efficiency, and  $N_p$  is the number of particles per unit volume. The total extinction efficiency,  $Q_{ext}(m(\lambda_o), D)$  is a function of the optical properties of the particles and suspending medium through the complex refractive index,  $m(\lambda_o)$ :

$$m(\lambda_o) = \frac{n(\lambda_o) + i\kappa(\lambda_o)}{n_o(\lambda_o)} \quad (2)$$

where  $n(\lambda_o)$  and  $\kappa(\lambda_o)$  represent the real and imaginary components of the complex refractive index of the particles and  $n_o(\lambda_o)$  represents the real refractive index of the suspending medium.

## INTERPRETATION MODEL

Under the assumption that the fundamental scattering model described in equations (1-2) applies, it is proposed to approximate the complex structure of microorganisms by dividing it into **M** groups or populations, each of which will be characterized by its corresponding scattering and absorption components. The

characteristic dimensions of each structure with its corresponding optical properties will largely define the scattering component, whereas the absorption component will be defined by the chemical composition of the structure, in particular by its chromophoric content. For example the following groups may be considered as distinct populations: the main body of the microorganisms, the cell wall, nuclei, mitochondria, and other internal structures such as inclusions, etc. The total scattering and absorption components of the spectrum will be given by the weighted sum of the contributions from the selected  $\mathbf{M}$  structures. Since it is not known a priori which absorption and/or scattering component will dominate, with this approach it is possible to formulate and test hypotheses as to the location and properties of chromophoric groups and scattering elements. Under the above approximations, the turbidity spectrum of a microorganism can be written in terms of  $\mathbf{M}$  distinct populations (37):

$$\tau(\lambda_0) = N_p \ell \left(\frac{\pi}{4}\right) \sum_{i=1}^{\mathbf{M}} x_i \int_0^{\infty} Q_{ext,i}(m_i(\lambda_0), D) D^2 f_i(D) dD \quad (3)$$

Where  $x_i$  ( $i = 1 \rightarrow \mathbf{M}$ ) is the number fraction corresponding to each population such that,

$$\sum_{i=1}^{\mathbf{M}} x_i = 1 \quad (4)$$

The real and imaginary parts of the complex refractive index are functions of the chemical composition and can be calculated as a weighted sum of the contributions from the chromophores within each population:

$$n_i = \sum_{j=1}^{N_i} \omega_{ij} n_{ij} \quad (5)$$

$$k_i = \sum_{j=1}^{N_i} \omega_{ij} k_{ij} \quad (6)$$

Where  $\omega_{ij}$  represents the mass fraction of  $j^{\text{th}}$  chromophore contained in the  $i^{\text{th}}$  population,  $n_i$  and  $k_i$  correspond to the real and imaginary refractive indices of each population, and  $N_i$  represents the total number of chromophoric groups in the  $i^{\text{th}}$  population.  $N_{\text{total}}$  corresponds to the sum of the chromophores present in all the structures. It is important to note that the additivity of the optical properties applies only within each population. Adding the scattering contributions represented by equations (3-6) closes the total mass balance for each chromophoric group. Assuming volume additivity, the total concentration can be readily calculated in terms of the concentration of each population or structure:

$$c_{\text{total}} = \sum_{i=1}^M c_i \quad (7)$$

Where  $c_i$  is the concentration of each population.

The diameter in equation (3) can be calculated from the closest geometrical approximation to the shape of the microorganisms (i.e., the diameter is calculated from the cell volume). For example, if the shape of a microorganism is approximated as a prolate ellipsoid (20-21), the volume equivalence for the ellipsoid and the sphere is given by:

$$V_e = \frac{4}{3}\pi ab^2 = \frac{\pi D^3}{6} = V_s \Rightarrow D \quad (8)$$

Where:  $V_e$  is volume of the ellipsoid,  $a$  and  $b$  are the major respectively minor lengths of the semi-axes of the ellipsoid,  $V_s$  is the volume of the sphere and  $D$  is the equivalent diameter of the microorganism.

## **MATERIALS AND METHODS**

### **Materials**

*E. coli* (JM 109ATCC #53323) and *Bacillus globigii* spores (ATCC #9372) were obtained from the American Type Culture Collection (ATCC) Manassas, Virginia. The n-acetyl/ethyl ester derivatives used as model molecules to represent chromophores imbedded in protein molecules were purchased from Sigma-Aldrich, Saint Louis Missouri. The dipicolinic acid was also from Sigma-Aldrich.

### **Spectroscopy measurements**

The Uv-vis transmission spectra from the model molecules and cell suspensions were recorded using a diode array spectrometer (HP 8443 Hewlett-Packard, Palo Alto, CA) having an acceptance angle smaller than  $2^\circ$ . All measurements were conducted at room temperature using a 1 cm pathlength cuvette. To illustrate the composition information, the first derivative of the spectra was numerically evaluated. The first derivative amplifies the presence of absorption bands related to the chromophoric (chemical) composition of the sample (37).

To obtain the extinction spectra of model molecules, stock solutions of the model molecules were prepared in phosphate buffers at several pH values and at physiological concentrations. The stock solution was diluted with buffer to suitable concentrations

(i. e., selected to yield optical density values below 1.2 Absorbance Units (Au)) and the spectra were recorded. A minimum of 5 dilutions were measured to obtain adequate estimates of the extinction coefficients. A least squares procedure was implemented to estimate the extinction coefficient at each wavelength (37).

The *Bacillus globigii* spores were directly suspended in sterilized de-ionized water and vortexed for few seconds prior to the spectroscopy measurements. Vegetative cells of *E. coli* were washed in sterilized de-ionized water according to the protocol described in Alupoaei (37). To eliminate concentration and particle number effects, the transmission spectra were normalized with the average optical density evaluated between 230-900 nm (37).

### **Scattering Calculations**

The Mie scattering coefficients in equation 3 were calculated with a computer program which includes multiwavelength spectral calculations and has been adapted to calculate distributions of particle sizes (37). This program has been extensively tested against available computer codes and published tables (25, 39). The refractive index of water  $n_o(\lambda_o)$  in Equation 2 as a function of wavelength was calculated from the correlation reported by Thormählen (40).

### **Spectroscopy Results**

Figures 1-2 show typical optical density spectra measured for *E. coli* cells and *Bacillus globigii* spores together with their first derivative spectra. Qualitative comparison of the multiwavelength transmission spectra of *E. coli* cells and *Bacillus globigii* spores reveals the sensitivity and discriminating power of the spectroscopy approach, as expected, the spectra of *E. coli* cells and *Bacillus globigii* spores are quite

different (1, 15, 19). Notice in the spectrum of *E. coli* the peak at approximately 260 nm, which is generally but not necessarily, attributed to the absorption of nucleic acids (6, 19, 30, 37). This band is not apparent in the spectrum of the spores. The spores, on the other hand, show features that can be attributed to the presence of dipicolinic acid (41) (see also Figure 5). These spectral fingerprints will be used as reference to test the sensitivity of the calculated spectra to the model parameters, and for the estimation of the refractive index of the microorganisms.

### **Estimation of Optical Properties**

Careful inspection of the chemical data reported for microorganisms (41) suggests that the majority of the dry mass is composed of proteins and organic matter with small or negligible absorption in the wavelength region of interest. Therefore, the optical properties necessary for the implementation of equations (3-8) have been divided into three categories, the average optical properties pertaining to the non-chromophoric scattering groups approximating the cell macrostructure, the average optical properties pertaining to the non-chromophoric scattering groups approximating the cell the internal structure, and the optical properties of known chromophoric groups within the cells. Within the context of the categories described above, non-chromophoric groups include molecules like polysaccharides, proteins, lipids and other biomolecules for which the contribution of chromophoric groups to their absorption spectra can be neglected.

The first set of properties is assumed to represent the bulk refractive index of the microorganism macrostructure (30). For this the Cauchy approximation to the real refractive index was used (41):

$$n_1(\lambda) = a_o + \frac{a_1}{\lambda^2} + \frac{a_2}{\lambda^4} + \dots \quad (9)$$

Equation 9, in two-parameter form, has been extensively used for representation of the refractive index wavelength dependence of non-chromophoric macromolecules (43), and it adequately represents the data reported for the refractive index of microorganisms (30). The Cauchy parameters for the bulk refractive index of microorganism macrostructure were estimated from the measured spectra (Figs 1-2) and the microorganism volume approximated by eqn. 8 from the dimensions determined by microscopy (37). A least squares iterative procedure was set up where a transmission spectrum was calculated with eqn. 1 in the spectral region where no chromophore absorption was expected (400-900 nm) and compared with the measured transmission spectrum at each wavelength. The procedure was repeated with new estimates of the refractive index parameters obtained using a standard Marquardt-Levenberg algorithm (37). This iterative procedure continued until convergence was achieved (i.e., relative changes in the sum of squares were less than  $10^{-6}$ ). The parameter values estimated from Figures 1-2 are given in Table I and yield refractive index estimates that are in good agreement with values reported in the literature.

The second set of optical properties corresponding to the refractive index parameters for the internal structure elements (Equation 9) were estimated under the assumption that primarily non-absorbing macromolecules compose the internal scattering elements (41). Analysis of the data reported in the literature in the form of specific refractive index increments of proteins, polysaccharides, etc. (43) resulted in the following average estimates:

$$n(\lambda_o) = 1.55 + \frac{5900}{\lambda_o^2} \quad (10)$$

The third category of optical properties corresponds to chromophoric groups that can be incorporated to defined scattering elements, or can scatter by themselves (i.e., DNA). These optical properties were estimated from measurements of the absorption coefficients of model molecules, and of measurements of the refractive index at 542 nm. To account for the protein content, and the concentration of other chromophoric groups such as DNA, RNA, and dipicolinic acid, model molecules representing the Uv-vis absorption characteristics of chromophoric amino acids and nucleotides were used (44). The chromophores imbedded in protein molecules have been represented with n-acetyl/ethyl ester derivatives of the aminoacids (44). Whenever possible, as in the case of dipicolinic acid, the actual chromophoric molecules were used. The spectra for the purine and pyrimidine bases were obtained from the data reported by Adams, Knowler and Leader at room temperature and pH=7 (45).

The dependence of the refractive index as function of wavelength was established through the use of the Kramers-Kronig transforms (7, 25, and 37). The optical properties of the three main chromophoric species, total nucleotides, a typical protein containing chromophoric aminoacids, and dipicolinic acid estimated with the procedures described above are shown in Figures 3-5. As it can be appreciated in Figure 4, the values of the optical properties of DNA calculated from the model molecules are in good agreement with the values reported in the literature (7).

## SENSITIVITY ANALYSIS

With the refractive index estimates for *E. coli* cells and *Bacillus globigii* spores (Table I and equation 10), and with the literature values of typical dimensions of the microorganisms and their chromophore content (Table II), the sensitivity of the calculated spectra (equation 3) to the size and composition of the scattering elements can be explored. To study the sensitivity of the model a computer program based on equations 3-7 has been implemented. This program enables the calculation of **M** monodisperse or polydisperse populations of scattering elements, and it allows for the chromophoric groups to be distributed among the populations selected. To explore the effect of variance of the particle size distribution within each population, a lognormal distribution has been used. The sensitivity of the predicted spectra to the model parameters has been studied by formulating a series of hypothesis concerning: the mean particle size and the variance of each population, the distribution of chromophores between the structures defined (equations 3-7), and by varying the number fraction for each population over a range of interest. The hypotheses formulated have been tested by comparing the spectral features predicted by the model with the features of the normalized measured spectra (Figs. 1-2). In comparing the measured and the calculated spectra it is important to note that the wavelength correlation is the key variable, not the amplitude of the spectra, which is dictated by the number of particles.

The first step in the exploration of the sensitivity of the predicted spectra to the model parameters consists in comparing the relative magnitude of the absorption coefficients of the main chromophoric groups. This is important in the context of equations 5-7. Note that the chromophore composition enters the model linearly in the calculation of the

optical properties of the scattering elements, but non-linearly in the calculation of the contribution from each scattering element.

Figure 6 shows a comparison of the absorption spectra from total nucleic acids, dipicolinic acid, and the main chromophoric aminoacids weighted by their typical relative concentrations (41). Notice that the contribution of the aminoacids to the total spectrum is rather small and for all practical purposes may be considered negligible (46). This leads to an important simplification because it suggests that it may be possible to represent the main spectral features of microorganisms with only a small set of chromophoric groups (37). Also, notice from Figure 4 that, the spectral differences between the nucleic acids are sufficiently small that, initially, a representative set of optical properties can be used for the evaluation of model (37).

If the effect of the concentration of chromophoric aminoacids is initially neglected, the total number of variables to explore is:  $M \times (N_{\text{total}} + 2) - 1$ , and includes, the average size and variance for each population, the number fraction of each population, and the total number of chromophores ( $N_{\text{total}}$ ) present in all the structures. The minimum number of structures is one (i.e.,  $M=1$ ). However, with one structure it was not possible to replicate the spectral features shown in Figures 1-2. The next logical step is to assume a contribution from the internal structure of the microorganisms (i.e.,  $M=2$ ), and to formulate the hypotheses concerning the distribution of chromophoric groups on this basis. The resulting number of variables for  $M=2$  and  $N_{\text{total}}=3$ , has been extensively explored by varying one parameter at the time (37); the results for relevant variable combinations are described below. For these, unless otherwise indicated, the main chromophoric groups have been assumed to be part of the microorganism macrostructure.

The effect of the microorganism size on the spectra is shown in Figure 7 for *E. coli* cells and in Figure 8 for *Bacillus globigii* spores, notice that the calculated spectra for both microorganisms replicate the spectral features of the measured spectra (see Figures 1-2 for comparison). As it can be readily appreciated, the size of the microorganism plays a definite role in defining the features across the spectrum. Similarly, the average size representing the internal structure elements has an important effect in the definition of spectral features, particularly at short wavelengths. It is also interesting to notice that, for the range of refractive index ratios estimated (Table I), and for the average sizes estimated for the internal structure (50-200nm), the effect of the variance of the size distribution on the calculated spectra is small. For example, changes in the variance of the lognormal distribution between 0-0.2, for particles with a mean diameter of 1  $\mu\text{m}$  and a refractive index of 1.388, result in differences smaller than 10% in the normalized optical density spectrum. The effect of the variance of the distribution for the internal structure is somewhat more pronounced given that the refractive index of the internal structure is higher, but it is small enough to justify using the mean size to explore the effect of the size of the internal structure on the spectra. This is further demonstrated in Figure 9 with the calculated spectra for *E. coli* cells. Because the size of the internal structure is relatively small (0.02-0.1  $\mu\text{m}$ ), the scattering effects are more pronounced at shorter wavelengths. The inset figure shows the contribution of the internal structure to the overall spectra.

Figure 10 shows the effect of changing the chemical composition by varying the dipicolinic acid content. As it can be observed, the spectral features due to the absorption bands of dipicolinic acid are clearly discernable. Notice that, although the amplitude of

the absorption bands is proportional to the changes in concentration (see the magnification in the inset Figure), the effect of the concentration on the spectra is non-linear. The reason for this is that the scattering of light is a non-linear function of the optical properties of the particles and therefore of the chemical composition (equations 1-2). Because of this non-linear dependence the association of the chromophoric groups with a particular scattering structure is important. Figure 11 shows the effect, on the simulated transmission spectra of *E. coli*, of associating the same concentration of nucleotides per cell with either the macrostructure or with the internal structure. In other words, the nucleotides will be considered alternatively part of the macrostructure or part of the internal structure. Note that the association of different chromophoric groups results in changes in the refractive index of the scattering structures and of the total refractive index of the microorganism. For example, the refractive index, at 542 nm, of the macrostructure without the nucleotides is 1.3879 and with nucleotides is 1.4059. Similarly, the refractive index of the internal structure with nucleotides is 1.5764 and without 1.5701. Notice that the internal structure with nucleotides will have higher contrast. It is evident that the overall refractive index will also be affected. In the first case the composite refractive index of the microorganism becomes 1.4518 whereas in the second case becomes 1.44068. Since the number of particles and the particle sizes are kept constant, a difference in optical density is obviously expected. As it is shown in Figure 11, these effects are apparent in the spectra.

The volume fraction and the size of the internal structure elements are also reflected in changes in the spectral features. Figure 12 shows the effect of changing the average size of the internal structure, at constant volume fraction, when the chromophoric groups

are associated with the internal structure. As in the case described in Figure 9, because the size of the internal structure is relatively small (see inset Figure), the scattering effects are more pronounced at shorter wavelengths. Comparison of Figures 9 and 12 demonstrate the differences arising from the location of the chromophoric groups. Figure 13 shows the effect of changing the volume fraction of internal scattering elements on the calculated spectra for *E. coli*, for a given size of the internal scattering elements. The inset figure shows the contribution of the volume fraction occupied by the internal structure to the overall spectra. Clearly, the model predicted spectra reflect the main features present in the measured spectra of both microorganisms. Furthermore, the sensitivity of the calculated spectra to the model parameters suggests that the proposed model can be used for the quantitative deconvolution of experimental data (37).

## **SUMMARY AND CONCLUSIONS**

A model for the interpretation of the multiwavelength Uv-vis spectra of microorganisms and cells has been formulated. The proposed interpretation model is based on light scattering theory, spectral deconvolution techniques, and on the approximation of the frequency dependent optical properties of the basic constituents of living organisms. The optical properties of chromophores known to be present in microorganisms have been evaluated and reported. The optical properties as functions of wavelength, and literature data on the size and chemical composition of *E. coli* cells and *Bacillus globigii* spores have been used to explore the sensitivity of the calculated spectra to the model parameters. By comparison with experimentally measured spectra it has been shown that the proposed model can reproduce the spectral features of these two very different microorganisms. The sensitivity of the spectra to the variables in the interpretation model parameters suggests that the proposed model can be used for the quantitative deconvolution of spectra in terms of critical parameters necessary for the detection and identification of microorganisms. Subsequent publications will report on applications of the model to the interpretation of the spectra of bacterium vegetative cells and spores, *Cryptosporidium* and other microorganisms of interest.

## **Acknowledgements**

The authors would like to acknowledge the support of Los Alamos National Laboratory, (Los Alamos National Laboratory is operated by the University of California for the US Department of Energy W-7406-ENG-36), the American Water Works Research Foundation and the Engineering Research Center (ERC) for Particle Science and Technology at the University of Florida through the National Science Foundation (NSF) grant #EEC-94-02989.

## REFERENCES

1. Bacon, C., J. B. Rose, K. Patten and L. H. Garcia-Rubio (1995) Quantitative classification of *Cryptosporidium* oocysts and *Giardia* cysts in water using Uv-vis spectroscopy, Proc. SPIE **2388**, 471-480.
2. Bronk, B. V., W. P. van de Merwe and D. R. Huffman (1991) Polarized Light Scattering as Means for Detecting Subtle Changes in Microbial Populations, in *Modern Techniques for Rapid Microbiological Analysis* (Edited by W. H. Nelson), pp. 171-197, VCH Publishers Inc., New York.
3. Cross, D. A. and P. Latimer (1972) Angular Scattering from *E. coli* Cells, *Applied Optics*, **11** (5), 1225-1228.
4. Dudley Bryant, F. and P. Latimer (1969a) Optical Efficiencies of large particles of arbitrary shape and orientation, *J. Colloid Interface Sci.* **30** (3), 291-304.
5. Dudley Bryant, F., B. A. Seibert and P. Latimer (1969b), Absolute Optical Cross-Sections of Cells and Chloroplasts, *Archives of Biochemistry and Biophysics* **135**, 79-108.
6. Freifelder, D. (1982) Chapter 14 (In *Physical Biochemistry* 2nd edition). W.H. Freeman and Company, pp. 504.

7. Inagaki, T., R. N. Hamm, E. T. Arakawa and L. R. Painter (1974) Optical and dielectric properties of DNA in the extreme ultraviolet, *J. Chem. Phys.* **61**, 4246-4250,
8. Koch, A. L. (1968) Theory of the Angular Dependence of Light Scattered by Bacteria and Similar-sized Biological Objects, *J. Theoret. Biol.* **18**, 133-156.
9. Koch, A. L. and E. Ehrenfeld (1968) The Size and Shape of Bacteria by Light Scattering Measurements, *Biochem. Biophys. Acta* **165**, 262-273.
10. Latimer, P. and E. Rabinowitch (1959) Selective Scattering of Light by Pigments *in vivo*, *Archives of Biochemistry and Biophysics* **84**, 428-441.
11. Latimer P. and C. A. Holmes Eubanks (1962) Absorption Spectrometry of Turbid Suspensions: A method for Correcting for Large Systematic Distortions, *Archives of Biochemistry and Biophysics* **98**, 274-285.
12. Latimer, P. and P. Barber (1977) Scattering by Ellipsoids of Revolution; A comparison of Theoretical Methods, *J. Colloid and Interface Sci.* **63** (2), 310-316.
13. Lopatin, V. N. and F. Ya. Sidko (1988) *Introduction to Optics of Cell Suspensions*, Moscow: Nauka.

14. Mattley, Y., G. Leparc, R. Potter and L. H. Garcia-Rubio (2000) Light scattering and absorption model for the quantitative interpretation of human blood-platelet spectral data, *Photochem. Photobiol.* **71** (5), 610-619.
15. Mattley, Y. and L. H. Garcia-Rubio (2000) Multiwavelength spectroscopy for the detection, identification and quantification of Cells, Proc. SPIE National Meeting, Boston, Massachusetts, November 5-8.
16. McRae, R., J. A. McClure and P. Latimer (1961) Spectral Transmission and Scattering Properties of Red Blood Cells, *Journal of the Optical Society of America* **51** (12), 1366-1372.
17. Mourant, J. R., M. Campolat, C. Brocke, O. Esponda-Ramos, T. M. Johnson, A. Matanock and J. P. Freyer (2000) Light scattering from cells: the contribution of the nucleus and the effects of proliferative status, *Journal of Biomedical Optics* **5** (2), 131-137.
18. Newman, C. D., B. T. Hebner and F. S. Allen (1991) A Polarization-Sensitive Multiparameter Light-Scattering Characterization of Bacteria, in *Modern Techniques for Rapid Microbiological Analysis* (Edited by W. H. Nelson), pp. 145-169, VCH Publishers Inc., New York, NY.
19. Waltham, C., J. Boyle, B. Ramey and J. Smit (1994) Light scattering and absorption caused by bacterial activity in water, *Appl. Opt.* **33**, 7536-7540.

20. Wyatt, P. J. (1968) Differential Light Scattering: a physical method for identifying living bacterial cells, *Appl. Opt.* **7**, 1879-1896.
21. Wyatt, P. J. and D. T. Phillips (1972) Structure of single bacteria from light scattering, *J. Theor. Biol.* **37**, 493-501.
22. Sambrook, J., E. F. Fritsch and T. Maniatis (1989) Spectrophotometric Determination of the amount of DNA and RNA, (In *Molecular Cloning* 2nd edition). Cold Springs Harbor Laboratory Press. Appendix E.5.
23. Veshkin, N. L. (1999) *Photonics of Polymers*, Moscow University Press.
24. Bigio, I. J. and J. R. Mourant (1997) Ultraviolet and visible spectroscopies for tissue diagnostics: Fluorescence spectroscopy and elastic light scattering spectroscopy, *Phys. Med. Biol.* **42**, 803-814.
25. Bohren, C. F. and D. F. Huffman (1983) *Absorption and Scattering of Light by Small Particles*. John Wiley and Sons, New York.
26. Ross, K. F. A. and E. Billing (1957) The water and Solid Content of Bacterial Spores and Vegetative Cells as Indicated by Refractive Index Measurements, *J. gen. Microbiol.* **16**, 418-425.
27. Kerker, M. (1969) *The Scattering of Light and Other Electromagnetic Radiation*. Pergamon Press, New York.

28. van de Hulst, H. C. (1957) *Light Scattering by Small Particles*. Wiley, New York.
29. Sethi, V., P. Biswas, R. M. Clark and E. W. Rice (1997) Evaluation of optical detection Methods for waterborne suspensions, *Journal AWWA* **89** (2), 98-112.
30. Tuminello, P. S., E. T. Arakawa, B. N. Khare, J. M. Wrobel, M. R. Querry and M. E. Milham (1997) Optical Properties of *Bacillus subtilis* from 0.2 to 2.5  $\mu\text{m}$ , *Applied Optics*. **36** (13), 2818-2823.
31. Yabushita, S., K. Wada, T. Inagaki, and T. Ito (1985) Photometric and photoacoustic measurement of the absorbance of microorganisms and its relation to the micro-organism-grain hypothesis, *Astrophys. Space Sci.* **117**, 401-406.
32. Yabushita, S., K. Wada, T. Takai, T. Inagaki, D. Young and E. T. Arakawa (1986) A spectroscopic study of the micro-organism model of interstellar grains, *Astrophys. Space Sci.* **124**, 377-388.
33. Aas, E. (1984) *Some Aspects of Light Scattering by Marine Particles*, Oslo: Institute of Geophysics.
34. Flatau, P. (1992) *Scattering by Irregular Particles in Anomalous Diffraction and Discrete Dipole Approximations*, Ph.D. Thesis, Colorado: Colorado State University.

35. Purcell, E. M. (1969) On the Absorption and Emission of Light by Interstellar Grains, *Astrophys. J.* **158**, 433-440, 1969
36. Reynolds, L. O. (1975) *Optical Diffuse Reflectance and Transmittance from an Anisotropically Scattering Finite Blood Medium*, Ph. D. Dissertation, University of Washington
37. Alupoaei, C. E. (2001) *Modeling of the Transmission Spectra of Microorganisms*, Master of Science Thesis, University of South Florida
38. Elicabe, G. E. and L. H. Garcia-Rubio (1988) Latex particle size distribution from turbidimetry using inversion techniques. *J. Colloid Interface Sci.* **129**, 192-200
39. Wiscombe, W. J. (1979) Mie scattering calculations: Advances in technique and fast, vector-speed computer codes, NCAR/TN-140 + STR, National Center for Atmospheric Research, Boulder, Colorado.
40. Thormählen I., J. Straub and U. J. Grigull (1985) Refractive index of water and its dependence on wavelength, temperature, and density. *J Phys Chem Ref Data*, **14**, 933-945.
41. Murrell, W. G. (1969) Chemical Composition of Spores and Spore Structures, in *The Bacterial Spores* (Edited by G. W. Gould and A. Hurst), Chapter 7, Academic Press., New York, NY.

42. Johnson, B. L. and J. Smith (1972) Refractive index and Densities of some Common Polymer Solvents, in *Light Scattering from Polymer Solutions* (Edited by M. B. Huglin), Chapter 2, Academic Press New York, NY.
43. Huglin, M. B. (1972) Specific Refractive index Increments, in *Light Scattering from Polymer Solutions* (Edited by M. B. Huglin), Chapter 6, Academic Press, New York, NY.
44. García-Rubio, L. H., C. A. Lopez-Menacho and S. Grossman (1993) Characterization of proteins during aggregation II: Use of model molecules for spectroscopy analysis. *Chem. Eng. Comm.* **122**, 85-101.
45. Adams, R. L., J. T. Knowler and D. P. Leader (1989) *The Biochemistry of Nucleic Acids*, 10th edition, McGraw Hill, New York. Manchester K. L. (1997) When are nucleic acids not nucleic acids? Problems with estimation of nucleic acid purity by UV absorbance. *Biochemical Education*, **25**(4), 214-215.

Table I. Refractive index estimates for the microorganism macrostructure (eqn. 9)

|           | Estimated values (300-900 nm) |                              | Literature values             |                     |
|-----------|-------------------------------|------------------------------|-------------------------------|---------------------|
|           | <i>E. coli</i>                | <i>B. globigii</i><br>spores | Vegetative cells <sup>1</sup> | Spores <sup>1</sup> |
| $a_0$     | 1.3776                        | 1.4993                       | -                             | -                   |
| $a_1$     | 3034.91                       | 4393.90                      | -                             | -                   |
| $n_{542}$ | 1.3879                        | 1.5142                       | 1.386                         | 1.52                |

Table II. Literature and calculated values (prolate ellipsoid approximation) of typical dimensions of the microorganisms and their chromophore content

| Microorganism             | Calculated values |                       | Literature values                                       |   |
|---------------------------|-------------------|-----------------------|---|---|
|                           | E. coli           | B. globigii<br>spores | E. coli   | B. globigii<br>spores                     |
| Dimensions, $\mu\text{m}$ | -                 | -                     | <sup>2</sup> width: 1.1-1.5<br><sup>2</sup> length: 2-6 | <sup>3</sup> <1                           |
| Volume, $\mu\text{m}^3$   | 1.26-7.06         | 0.51-1.00             | <sup>4</sup> 1  | <sup>5</sup> 0.17-0.718                   |
| Equivalent diameter       | 1.34-2.38         | 0.99-1.24             | -   | -   |
| RNA g/cell                | -                 | -                     | -   | <sup>5</sup> 12.1-100.2x10 <sup>-16</sup> |
| DNA g/cell                | -                 | -                     | -   | <sup>5</sup> 5.0-20.8x10 <sup>-16</sup>   |
| DNA+RNA g/cell            | -                 | -                     | <sup>4</sup> 7x10 <sup>-14</sup>                        | 17.1-121x10 <sup>-16</sup>                |
| DPA, % dry weight         | -                 | -                     | -   | <sup>6</sup> 5.6-13.55                    |

<sup>1</sup>*B. cereus*, Ross and Billing, 1957

<sup>2</sup>Values from Bergey's Manual

<sup>3</sup>Values from Los Alamos National Laboratory

<sup>4</sup><http://esg-www.mit.edu:8001/esgbio/cb/ecoli.html>

<sup>5</sup>Doi, 1969, in *The Bacterial Spore*, pp 131

<sup>6</sup>Murrell, 1969, in *The Bacterial Spore*, pp 250

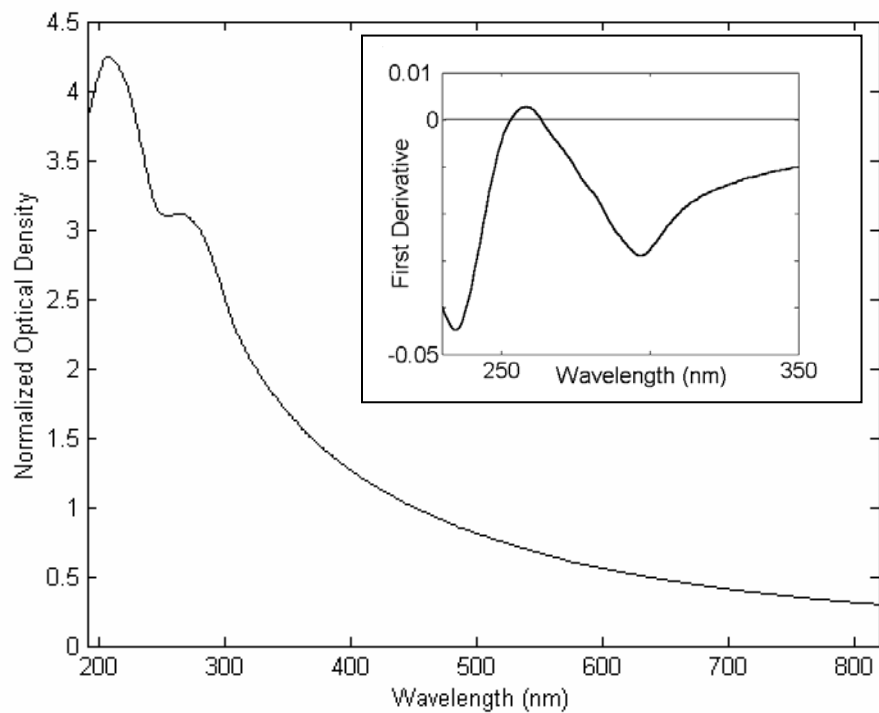


**Figure 1.** Typical measured Uv-vis spectra replicates of *E. coli* cells; the inset plot is the first derivative of the optical density spectrum

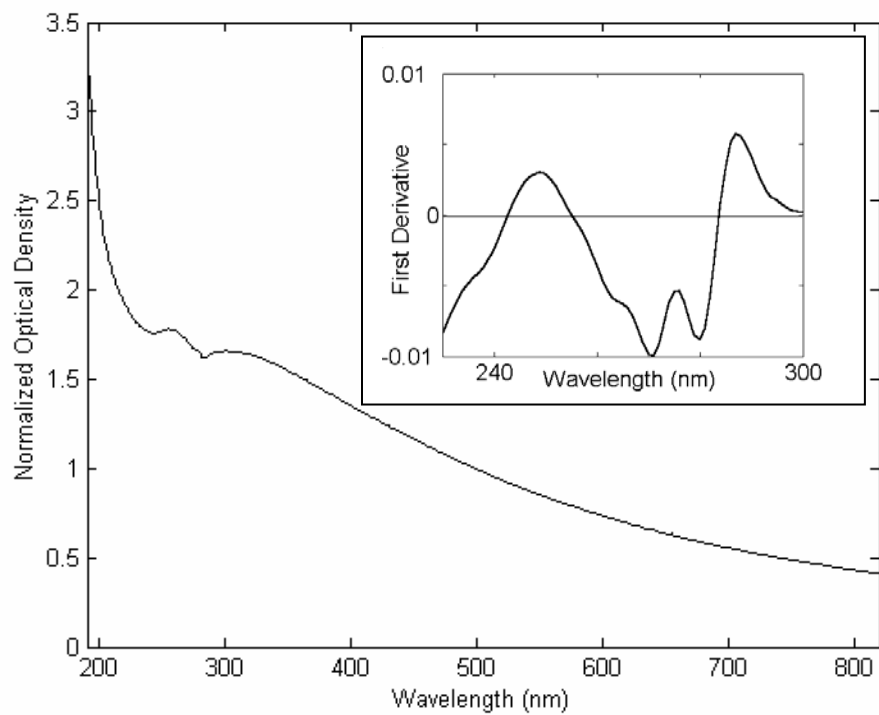


**Figure 2.** Typical measured Uv-vis spectra replicates of *B. globigii* spores, the inset plot is the first derivative of the optical density spectrum

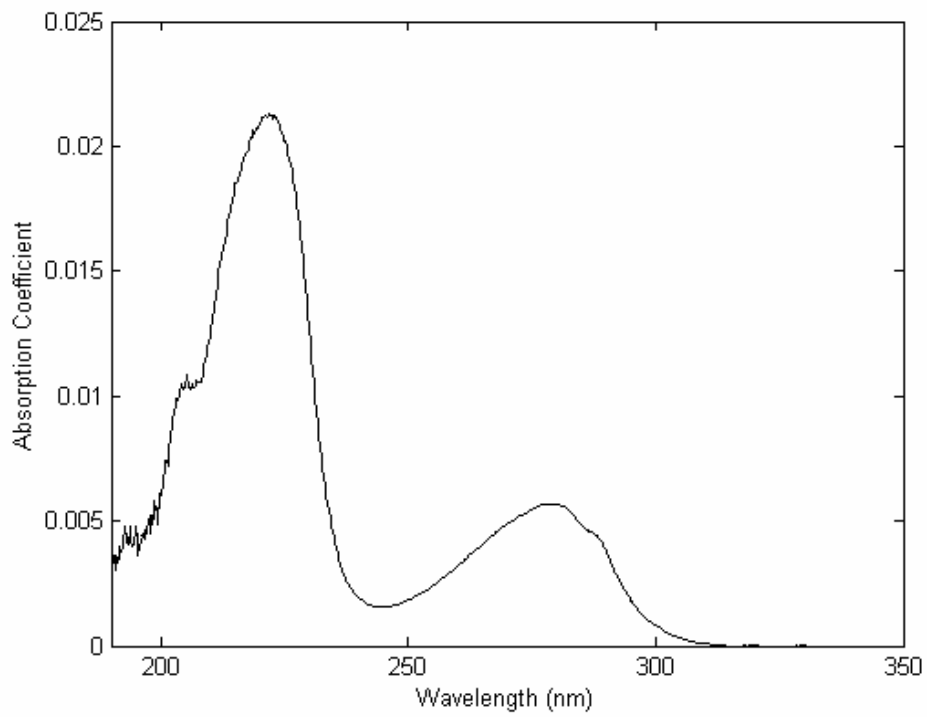


**Figure 3.** Absorption coefficient of an artificial protein containing chromophoric aminoacids in proportions reported for *B. subtilis* (Murrell, 1969)

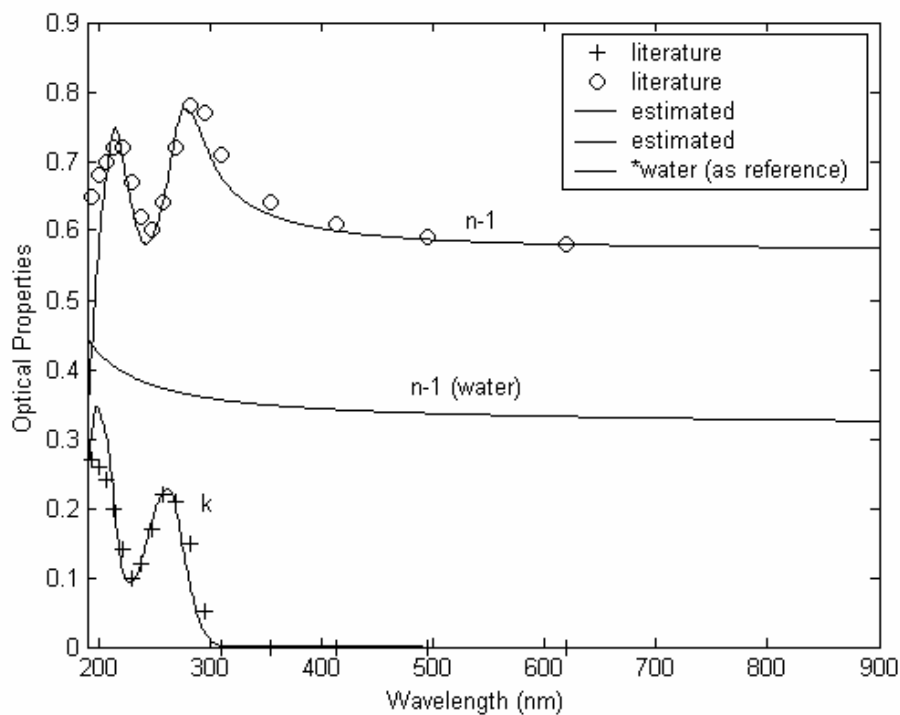


**Figure 4.** Comparison of the optical properties estimated for DNA from *E. coli* with the measured optical properties of DNA from calf thymus as reported by Inagaki et al, 1974. The estimated properties were corrected for moisture content.

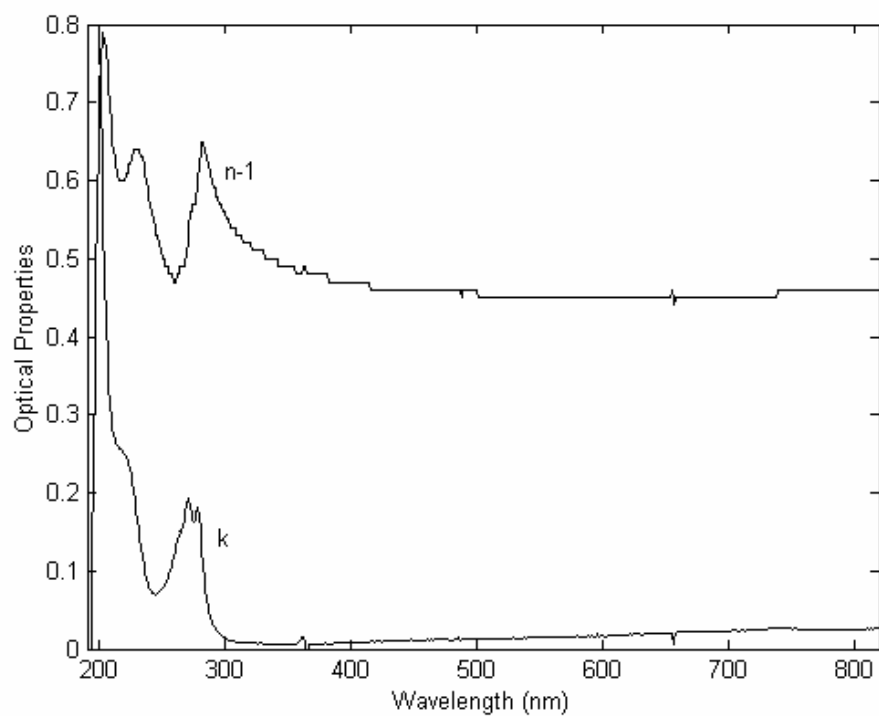


**Figure 5.** Optical properties of Dipicolinic acid, the inset plot is the first derivative of the absorption coefficient

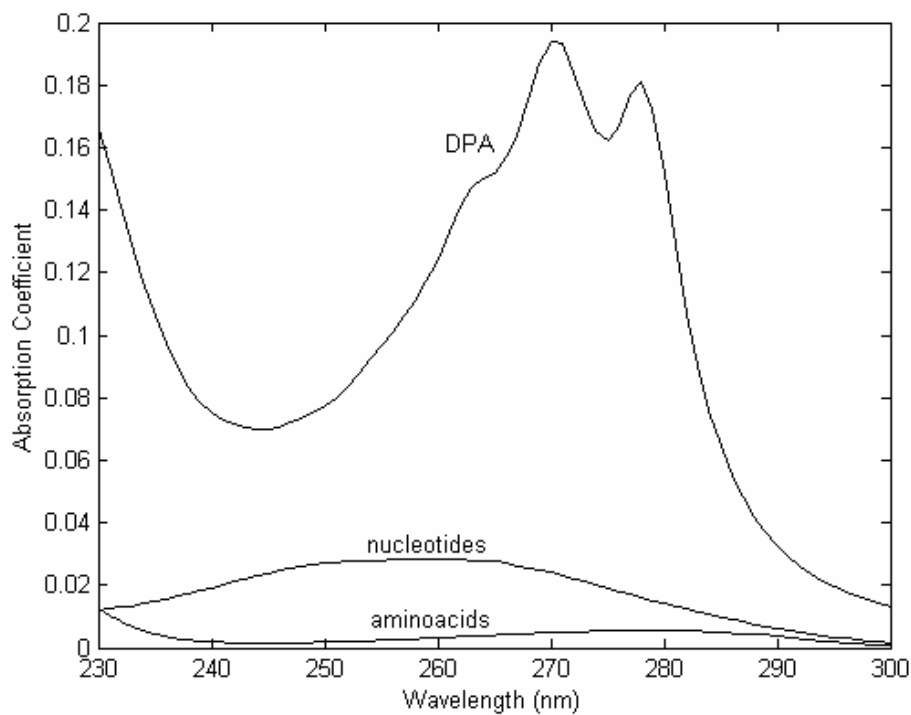


**Figure 6.** Comparison of the absorption coefficient of the total nucleic acid, chromophoric aminoacids, and dipicolinic acid weighted by their typical concentration in microorganisms (Murrell, 1969)

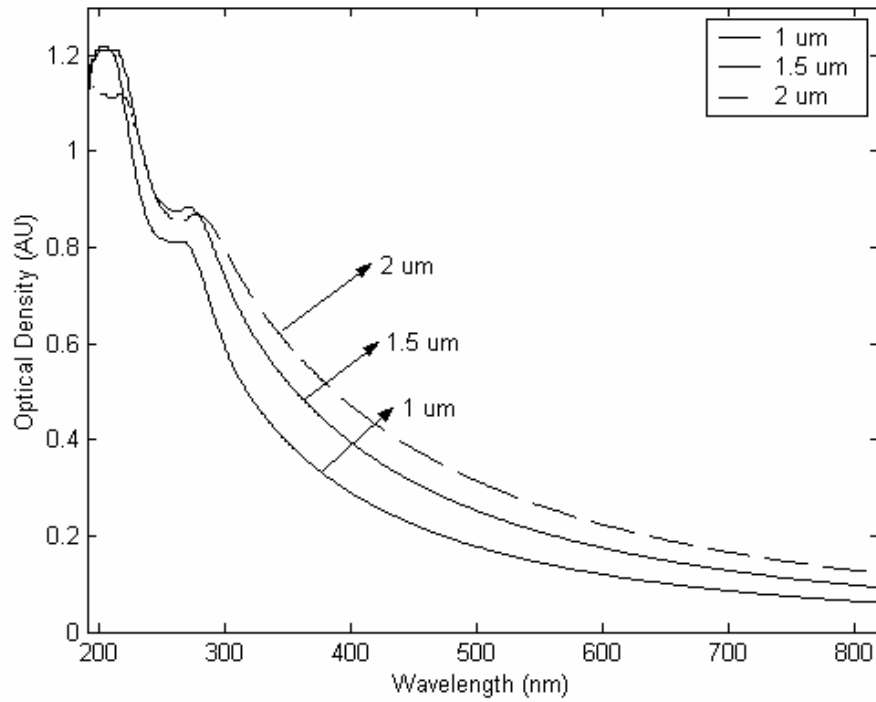


**Figure 7.** Effect of the microorganism size on the calculated spectra of *E. coli* cells. The nucleotides are associated with the macrostructure (compare with Figure 1). The chemical composition is given in Table II. The volume fraction occupied by the internal structure is 0.28 and the average size of the internal structure is 80 nm.

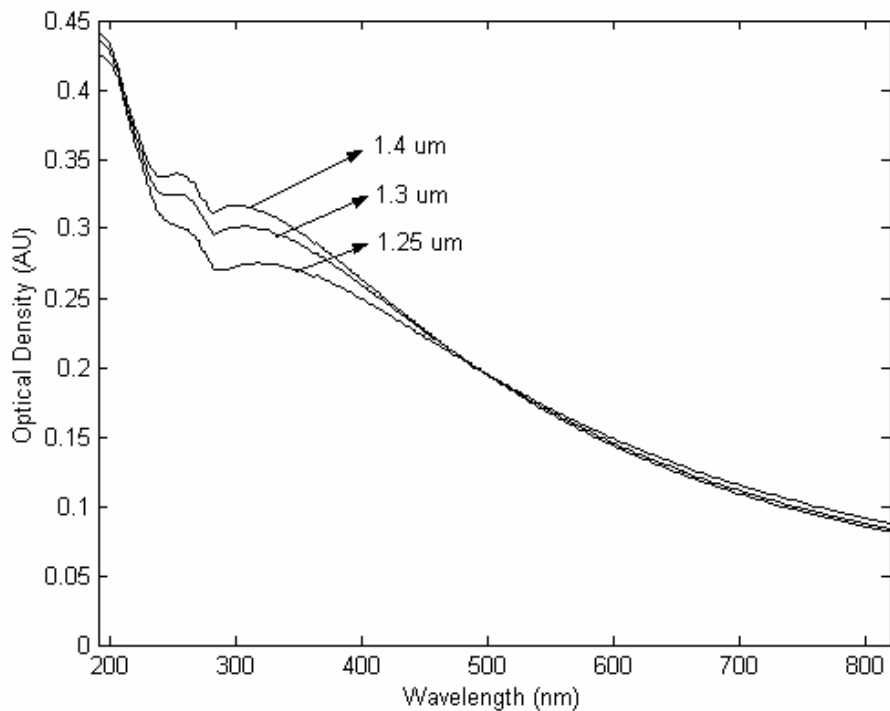


**Figure 8.** Effect of the microorganism size on the calculated spectra of *B. globigii* spores.

The dipicolinic acid is associated with the macrostructure (compare with Figure 2). The chemical composition is given in Table II. The volume fraction occupied by the internal structure is 0.41 and the average size of the internal structure is 132 nm.

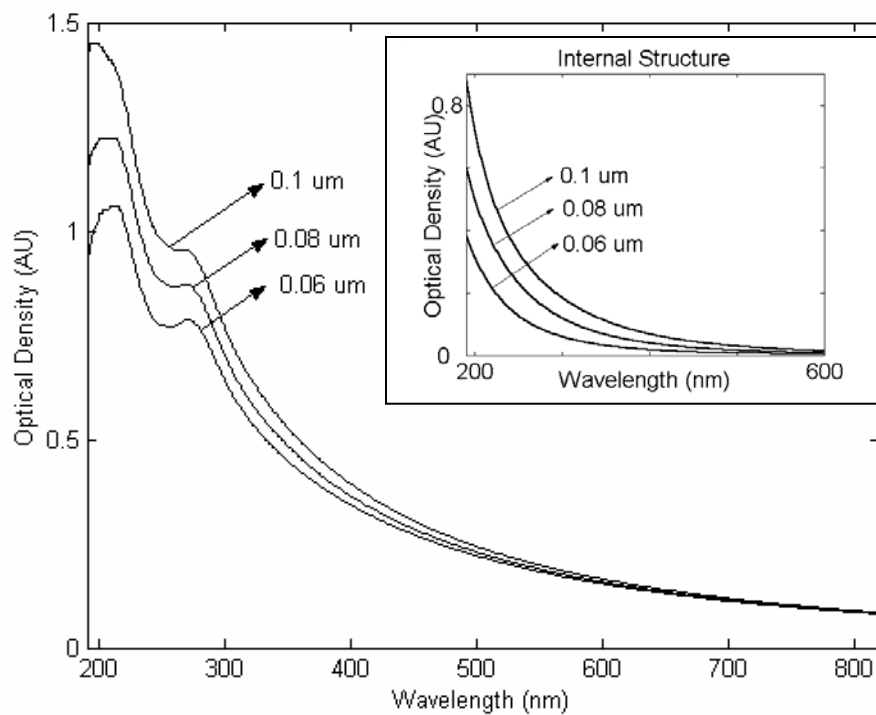


**Figure 9.** Effect of the average size of the internal structure on the calculated spectra of *E. coli* cells. The chromophores are associated with the macrostructure (compare with Figure 1). The chemical composition is given in Table II. It is assumed that the volume fraction occupied by the internal structure is 0.28 and the average size of the microorganism is 1.34  $\mu\text{m}$ .

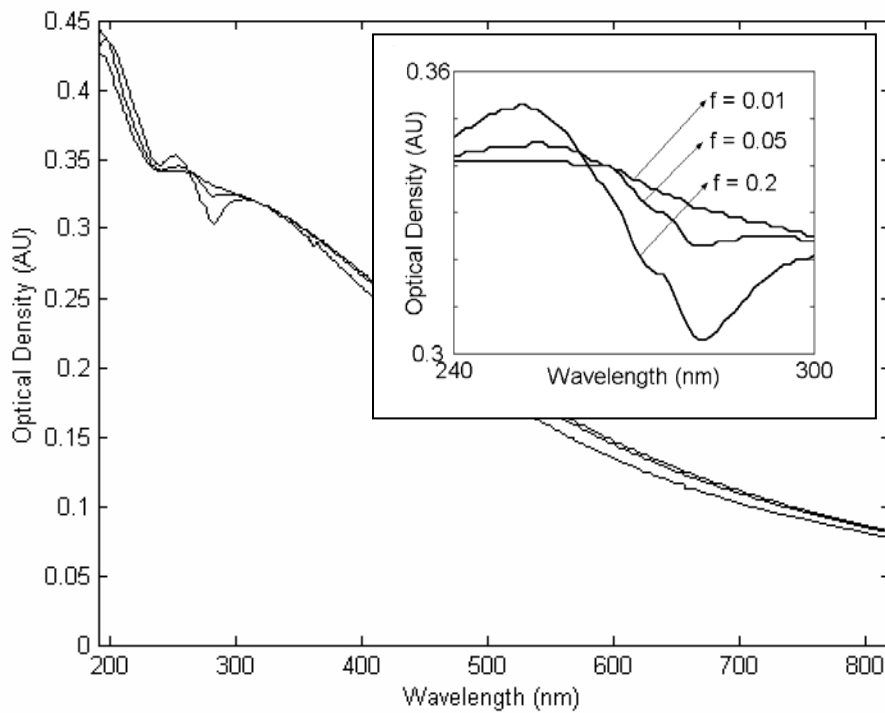


**Figure 10.** Effect of changing the chemical composition on the calculated spectra of *B. globigii* spores. Notice the spectral features due to the absorption bands of dipicolinic acid. It is assumed that the volume fraction occupied by the internal structure is 0.41, the size of the microorganism is 1.14  $\mu\text{m}$  and the average size of the internal structure is 132 nm.

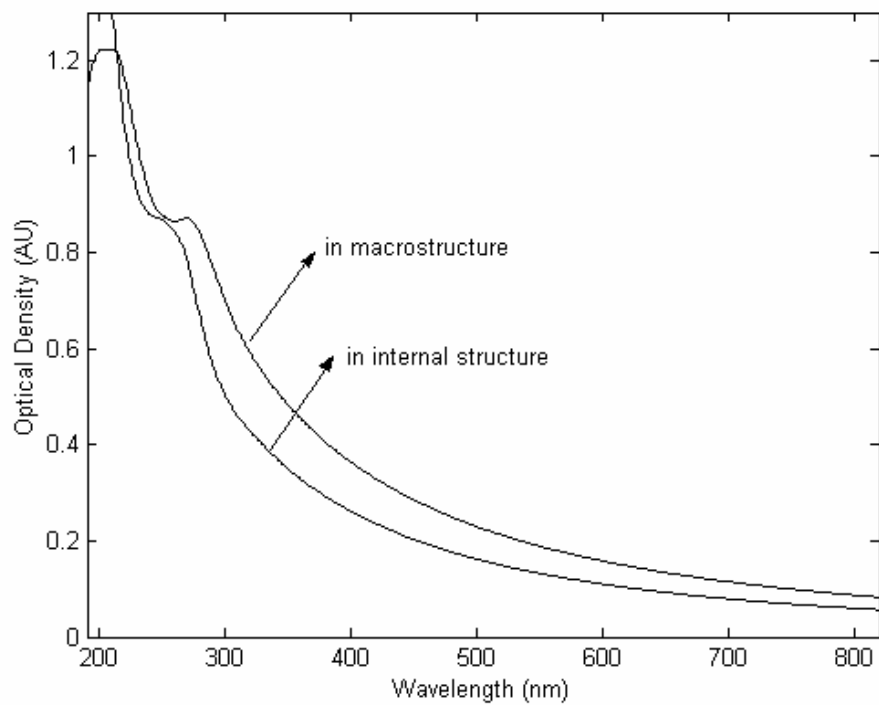


**Figure 11.** Effect of the location of the chromophoric groups on the calculated spectra of *E. coli* cells. The concentration of nucleotides per cell is kept constant. It is assumed that the volume fraction occupied by the internal structure is 0.28, the average size of the internal structure is 80 nm, and the size of the microorganism is 1.34  $\mu\text{m}$ .

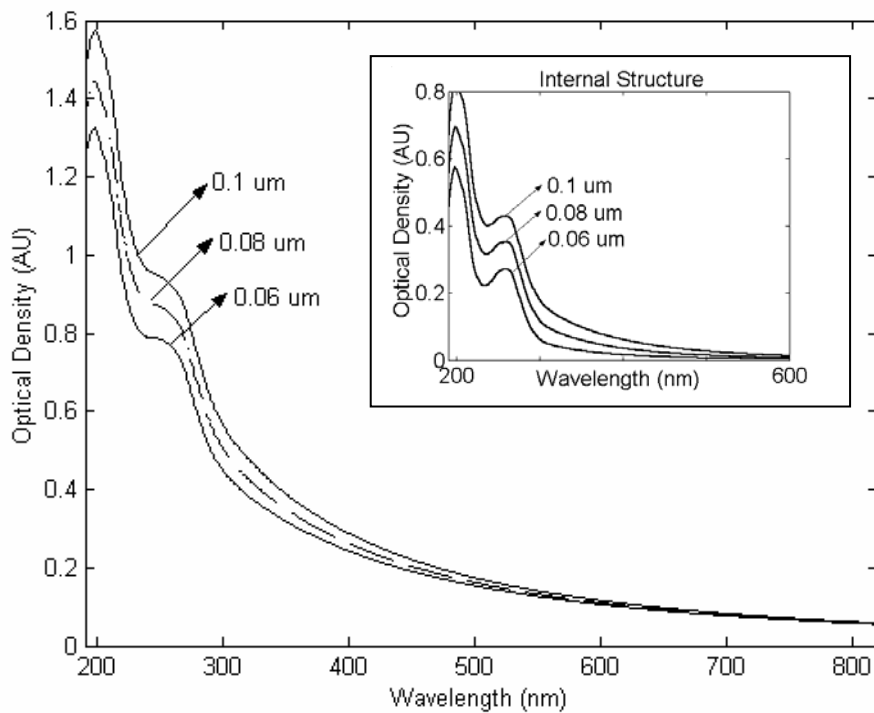


**Figure 12.** Effect of the average size of the internal structure on the calculated spectra of *E. coli* cells. The inset shows the contribution of the internal structure as function of its average size. For these spectra: the chromophores are associated with the internal structure (compare with Figure 9.), the concentration of nucleotides per cell is kept constant, and it is assumed that the volume fraction occupied by the internal structure is 0.28, and the size of the microorganism is 1.5  $\mu\text{m}$ .

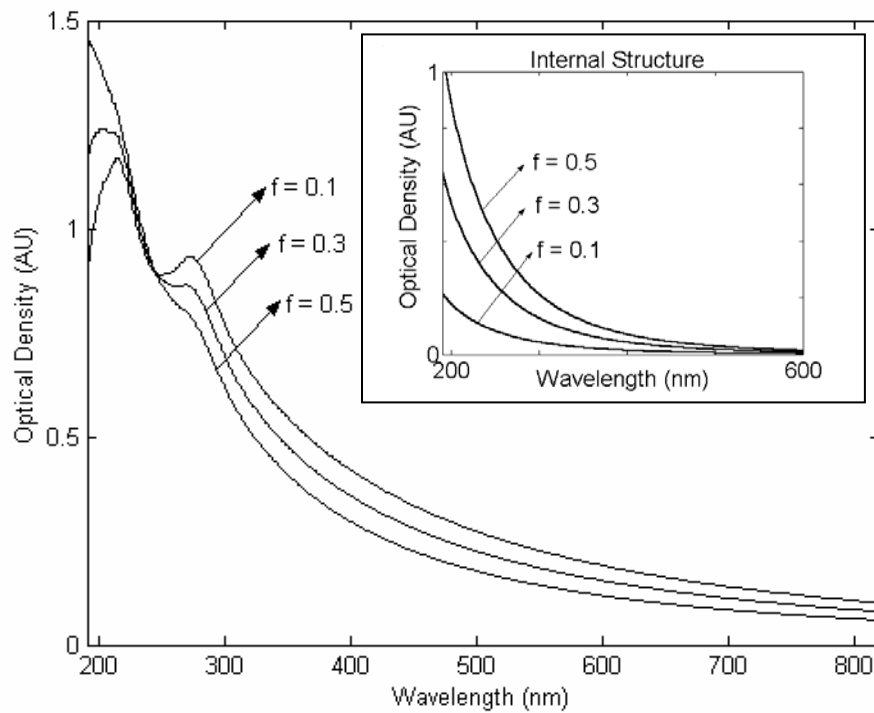


**Figure 13.** Effect of the volume fraction occupied by the internal structure on the calculated spectra of *E. coli* cells. The inset shows the contribution of the internal structure as function of its volume fraction. For these spectra: the chromophores are associated with the macrostructure, the chemical composition is given in Table II, and it is assumed that the average size of the internal structure is 80 nm, and the size of the microorganism is 1.34  $\mu\text{m}$ .